RNA Catalytic Properties of the Minimum (−)sTRSV Sequence

Arnold Hampel* and Richard Tritz

Plant Molecular Biology Center and Departments of Biological Sciences and Chemistry, Northern Illinois University, DeKalb, Illinois 60115

Received January 23, 1989; Revised Manuscript Received March 8, 1989

ABSTRACT: We have identified an RNA catalytic domain within the sequence of the 359 base long negative-strand satellite RNA of tobacco ringspot virus. The catalytic domain contains two minimal sequences of satellite RNA, a 50-base catalytic RNA sequence, and a 14-base substrate RNA sequence. The catalytic complex of catalytic RNA/substrate RNA represents a structure not previously found in any RNA catalytic reaction described to date. The reaction is truly catalytic since the catalytic RNA has multiple substrate cleavage events and is not consumed during the course of the reaction. A linear relationship is seen between reaction rate and catalytic RNA concentration. The reaction has a K_m of 0.03 μM, a k_{cat} of 2.1/min, a temperature optimum of near 37 °C, and an energy of activation of 19 kcal/mol.

Among the small plant viral satellite, virusoid, and viroid self-cleaving RNAs as well as the transcript from newt satellite DNA, the "hammerhead" self-cleaving catalytic cassette has been described (Forster & Symons, 1987; Uhlenbeck, 1987; Bruening et al., 1988; Cech, 1987; Epstein & Gall, 1987). An exception to this catalytic structure, however, is the 359-base autocatalytic RNA of tobacco ringspot virus [(−)sTRSV]. No sequences near the catalytic site can be put in the hammerhead configuration (Forster & Symons, 1987). This also appears to be the case for the antigenomic RNA of human hepatitis delta virus (Sharmeen et al., 1988). All these RNAs cleave to give 2′,3′-cyclic phosphate and 5′-OH termini (Buzayan et al. 1986a).

The (−)sTRSV has been shown to undergo both autocatalytic cleavage and ligation (Gerlach et al., 1986; Buzayan et al., 1986b). The cleaved RNA has a 5′-fragment that terminates in a 2′,3′-cyclic phosphate at adenine 49 and a 3′-fragment with a newly formed 5′-OH at guanine 48. The reverse reaction forms a normal 3′–5′ ApG bond (Buzayan et al., 1986c).

We now show the catalytic domain of this molecule consists of an RNA catalyst 50 bases long that efficiently cleaves an RNA substrate containing 14 bases of satellite RNA sequence. The 50-base RNA is a true catalyst since it has multiple turnover and it is not consumed during the course of the reaction. The substrate RNA is cleaved during the course of the reaction at the expected ApG bond to produce the expected 5′-fragment terminating at the base A with a 2′,3′-cyclic phosphate and a 3′-fragment terminating at the base G with a 5′-OH. The reaction has a temperature optimum of 37 °C, K_m = 0.03 μM, and k_{cat} = 2.1/min, and the velocity of reaction is proportional to the catalytic RNA concentration. No structure in this catalytic domain resembles that of the hammerhead.

Materials and Methods

Computer Modeling. The 359-base RNA sequence of (−)sTRSV (Buzayan et al., 1986a) was modeled with the University of Wisconsin Genetics Computer Group program FOLD (5/6/86). This program uses the methods of Zucker and Stiegler (1981) and Devereux et al. (1984) to calculate the minimum energy of the entire folded structure. The base numbering scheme is that of (+)sTRSV with the 5′–3′ direction being that of decreasing base number.

Preparation of RNA. RNAs were transcribed according to the T7 RNA polymerase transcription method on synthetic single-stranded DNA templates that are double stranded at the promoter site (Milligan et al., 1987). Synthetic DNA was made with phosphoramidite chemistry on the Northern Illinois University DNA synthesizer (Applied Biosystems 381A). Template DNAs were

catalytic RNA R51

3′-ATTATGCTGAGTGATATC^{+1}TTTGTCTCTTCAG-
TTGGTCTCTTTGTGTGCAACACCATATAATGGA-
CCAT-5′

substrate RNA S17

3′-ATTATGCTGAGTGATATATC^{+1}GCACTGTCAG-
GACAAA-5′

We hybridized either an 18mer or a 16mer DNA complement to the promoter on the template strand by heating an equimolar amount of template DNA with promoter complement to 65 °C for 3 min then by placing the mixture in ice. A typical transcription reaction used 8 ng/μL DNA template, 0.5 mM of each NTP, 2 mM spermidine, 40 mM Tris, pH 7.5, 4% poly(ethylene glycol) 6000, 6 mM $MgCl_2$, 4 mM NaCl, 10 mM dithiothreitol, 0.01% Triton X-100, 2.4 units/μL RNasin, 1.8 μCi/μL [α-^{32}P]CTP, and 3 units/μL T7 RNA polymerase (U.S. Biochemicals) and was run at 37 °C for 90 min. In vitro transcribed RNAs were isolated on 7 M urea–20% acrylamide gels for S17 substrate RNA and on 15% acrylamide gels for R51 catalytic RNA; the bands were cut out, isolated, quantitated by Cerenkov counting with appropriate standards, and redissolved in 10 mM Tris, pH 7.5, and 1 mM EDTA.

RNA Catalytic Reaction. The reaction of catalytic RNA cleaving substrate RNA was carried out by sequential addition to a tube of water, 4× reaction mix, substrate RNA, and catalytic RNA. The RNA had been previously heated to 65 °C for 2 min and cooled in ice. The 4× reaction mix gave a final 1× concentration in the reaction of 40 mM Tris, pH 7.5, 12 mM $MgCl_2$, and 2 mM spermidine.

Characterization of RNA. The RNAs R51 and S17 were sequenced according to standard methods (Donis-Keller et al., 1977). These methods also gave the 5′-terminal base. Terminal bases at the 3′-end were determined by ligation of the RNA to [5′-^{32}P]pCp with T4 RNA ligase (BRL methods

* Address correspondence to this author.

0006-2960/89/0428-4929$01.50/0 © 1989 American Chemical Society

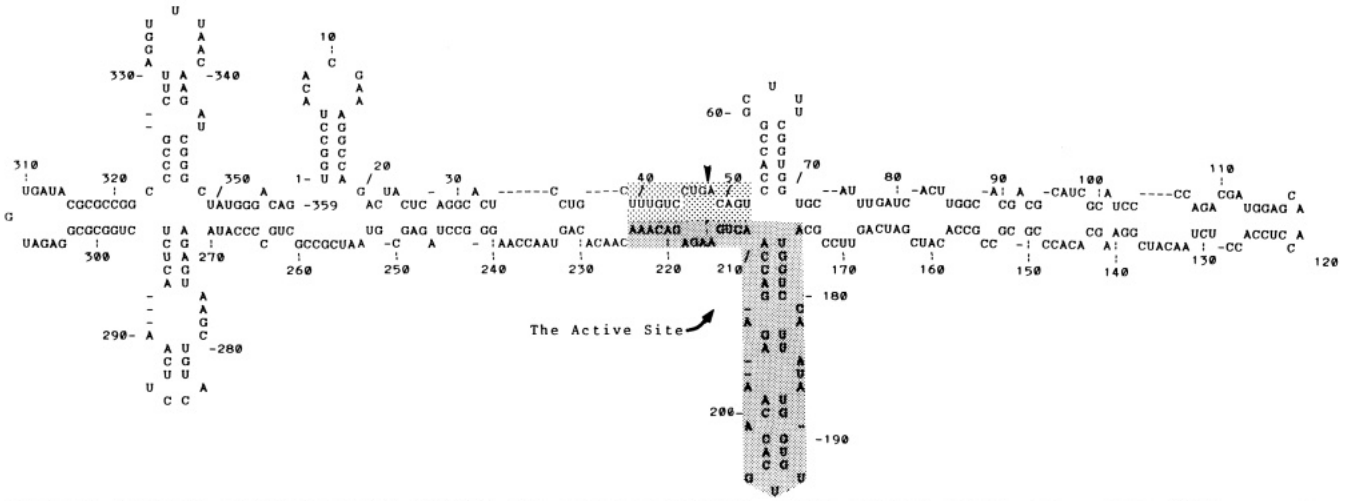

FIGURE 1: Minimum energy folding of (−)sTRSV. The molecule was folded with the Wisconsin RNA program FOLD with base numbers corresponding to (+)sTRSV (Buayan et al., 1986a). With this numbering scheme the 5′–3′ direction of the molecule is with decreasing base number. The minimum self-cleaving domain is identified: (top stippled area) substrate RNA sequence; (bottom stippled area) catalytic RNA sequence. The arrow is the site of cleavage.

manual), nuclease T2 digestion, and separation of labeled bases by PEI thin-layer chromatography in 0.3 M LiCl with appropriate standards.

The cleaved 5′-fragment (5′F) was identified by cleaving γ-^{32}P-labeled S17 with R51 and separating the cleavage products on acrylamide gels with RNA standards. Only one cleavage product contained radioactivity, and it migrated with the eight-nucleotide standard as predicted for the 5′F. The cleaved 3′-fragment (3′F) was identified by 5′-end labeling with [γ-^{32}P]ATP and polynucleotide kinase, nuclease P1 digestion, and separation by thin-layer chromatography in 0.4 M LiCl with appropriate standards. All RNA sequences corresponded to that expected from the synthesized DNA templates.

Migration of the 3′F was also compared to the RNA standard hydrolysis ladder, and migration was as expected for a 9mer without any terminal phosphates at all.

RESULTS

Identification of the Catalytic Domain. Figure 1 shows the minimum energy folding of the 359 base long plant satellite RNA (−)sTRSV sequence from the Wisconsin Genetics Computer Group program FOLD. The site of intramolecular cleavage undergone by the molecule at the ApG shown identifies those two bases of the substrate sequence. From the folding patterns of the resulting model, it is possible to identify sequence regions which may constitute a putative catalytic center of the molecule. We tested a large number of sequences which might constitute such a substrate region and catalytic region in a bimolecular reaction. The minimum sequences that carried out the most efficient reactions are those identified at the catalytic site in Figure 1. These are a 14-base substrate (bases 53–40) and a 50-base catalytic RNA (bases 224–175). The substrate RNA and the catalytic RNA have the following sequences:

substrate RNA

5′-UGACAGUCCUGUUU-3′

catalytic RNA

5′-AAACAGAGAAGUCAACCAGAGAAACACACG-
UUGUGGUAUAUUACCUGGUA-3′

The Reaction. RNA transcripts of both catalytic RNA and substrate RNA were prepared from synthetic DNA templates with T7 RNA polymerase. The catalytic RNA was a 51 base long RNA transcript (R51), which had the 50-base catalytic RNA sequence plus one additional vector base (G at the 5′-end), and the substrate RNA was a 17-base RNA transcript (S17), which had the 14 bases of substrate satellite RNA plus vector bases (GCG at the 5′-end). These two RNAs were mixed under reaction conditions and allowed to react. The cleavage products were the corresponding 5′-fragment (5′F) and 3′-fragment (3′F). The reaction is summarized as

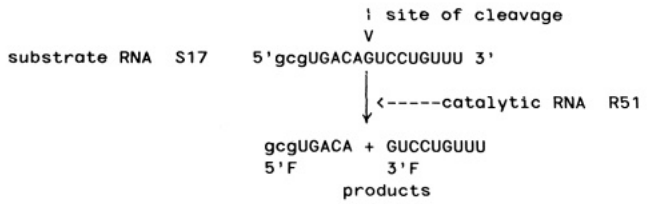

Cleavage of substrate occurred at 37 °C in 40 mM Tris buffer, pH 7.5, with magnesium and spermidine as counterions. Table I shows the dependence of the reaction rate on $MgCl_2$. Concentrations up to 20 mM were tested with the reaction rate continuing to increase. In the complete absence of counterion, no reaction occurred. The pH dependence for the reaction

Table I: Effect of Mg^{2+} and pH on Rate of Cleavage of RNA Substrate S17 by RNA Catalyst R51

	$t_{1/2}$ (min)
$[MgCl_2]$ (mM)[a]	
0	no detectable product
4	136
6	111
8	115
10	88
12	81
15	74
20	62
pH[b]	
5.5	330
6.0	120
6.5	67
7.0	48
7.5	42
8.0	38

[a] Substrate S17 concentration was 0.14 μM, and RNA catalyst R51 concentration was 0.0015 μM. Reactions were at 37 °C in 40 mM Tris, pH 7.5. [b] Substrate S17 concentration was 0.062 μM, and RNA catalyst R51 concentration was 0.0014 μM. Reactions were at 37 °C in 12 mM $MgCl_2$ and 2 mM spermidine with a buffer of 40 mM Tris for pH 7.0, 7.5, and 8.0 and of 40 mM Pipes for pH 5.5, 6.0, and 6.5.

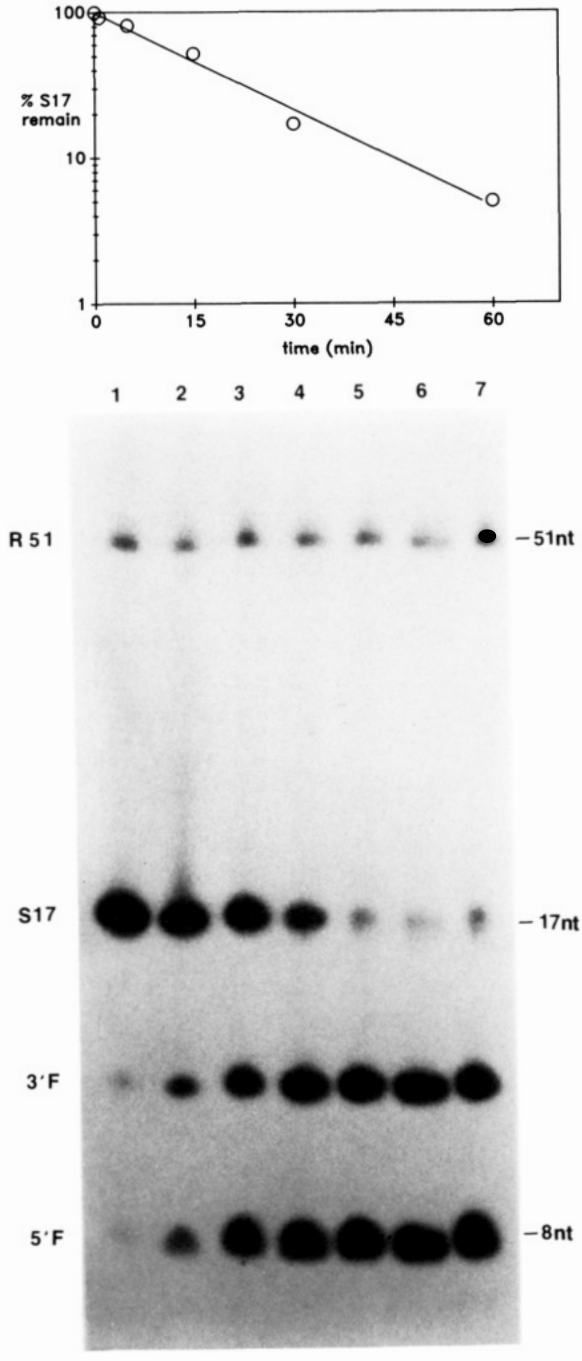

FIGURE 2: Time course of substrate S17 cleavage by catalytic RNA R51. The reaction was carried out at 37 °C in 12 mM $MgCl_2$, 2 mM spermidine, and 40 mM Tris, pH 7.5, at the following times: (lane 1) 30 s; (lane 2) 5 min; (lane 3) 15 min; (lane 4) 30 min; (lane 5) 60 min; (lane 6) 90 min; (lane 7) 150 min. The zero time point shown in the graph corresponds to no detectable product seen upon electrophoresis when S17 and R51 are incubated separately or when they are incubated only in the presence of 40 mM Tris, pH 7.5, as seen in Table I. Concentrations were [R51] = 0.0032 μM and [S17] = 0.09 μM. RNA was separated on 7 M urea–20% acrylamide gels; bands cut out and counted in the liquid scintillation counter for Figure 2–5. The migration of standards is shown. All species migrate as predicted. S17 is 17 nucleotides long as shown by sequencing and an S17 hydrolysis ladder. The 5′F moves with an eight-nucleotide species from the hydrolysis ladder as expected, and the 3′F moves nearly three bands slower than the corresponding 5′-triphosphate–3′-phosphate species in the hydrolysis ladder because the 3′F has no phosphate termini of any kind.

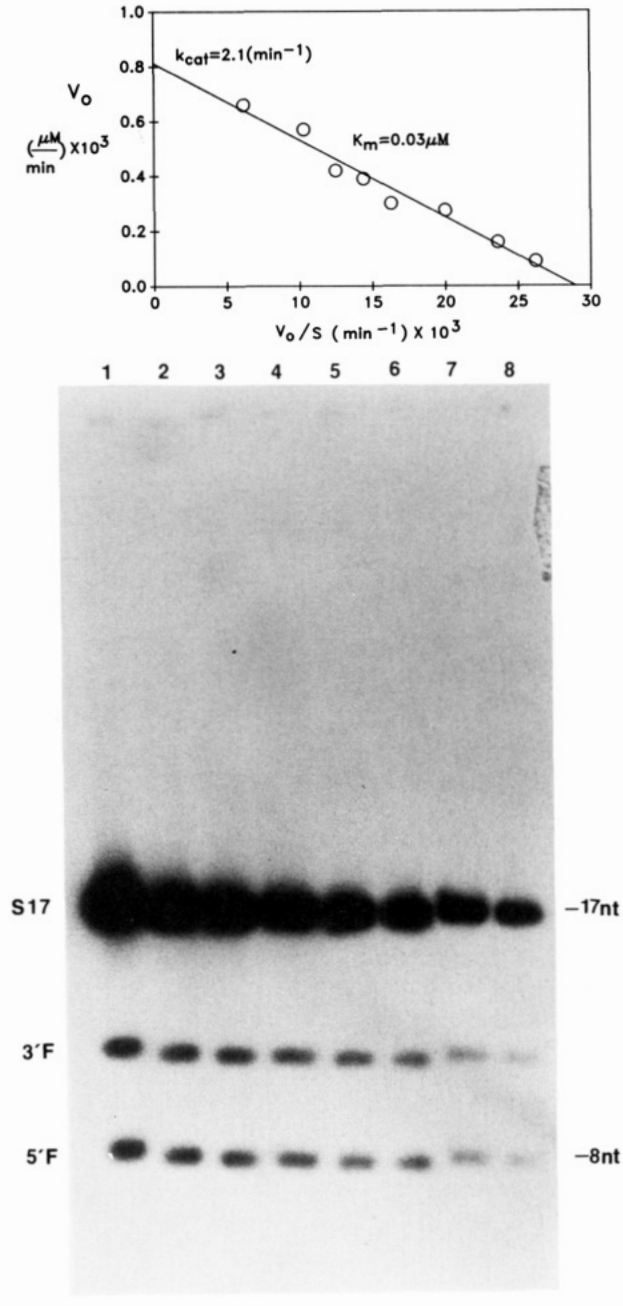

FIGURE 3: Eadie–Hofstee plot of catalytic RNA R51 cleavage of substrate RNA S17. The reaction was carried out at 37 °C in 12 mM $MgCl_2$, 2 mM spermidine, and 40 mM Tris, pH 7.5. Concentrations were as follows: [R51] = 0.0004 μM; [S17] = 0.125 (lane 1), 0.0625 (lane 2), 0.0417 (lane 3), 0.031 (lane 4), 0.021 (lane 5), 0.0156 (lane 6), 0.0078 (lane 7), and 0.0039 μM (lane 8). The concentration of R51 is too low to detect under these exposure conditions and is thus not identified in the gels.

rate is shown in Table I. Note that the reaction rate increases with increasing pH as one would expect for a base-catalyzed reaction. However, the effect of pH is masked by the catalytic activity of the RNA. A 100-fold increase in [OH^-] between pH 6.0 and pH 8.0 results in only a 3-fold increase in reaction rate of the RNA-catalyzed reaction.

Figure 2 shows the time course for this reaction with a substrate/RNA catalyst ratio of 30/1. The shape of the curve is similar to that of a typical enzyme-catalyzed reaction. Note that cleavage proceeds to virtual completion during the course of the reaction with only 2% of the substrate remaining after 150 min. This shows the RNA catalyst R51, of necessity, interacts with multiple substrate molecules during the course of the reaction. In addition, it is unaltered during the reaction and is completely recovered, showing that the R51 catalytic RNA sequence is truly a catalytic entity.

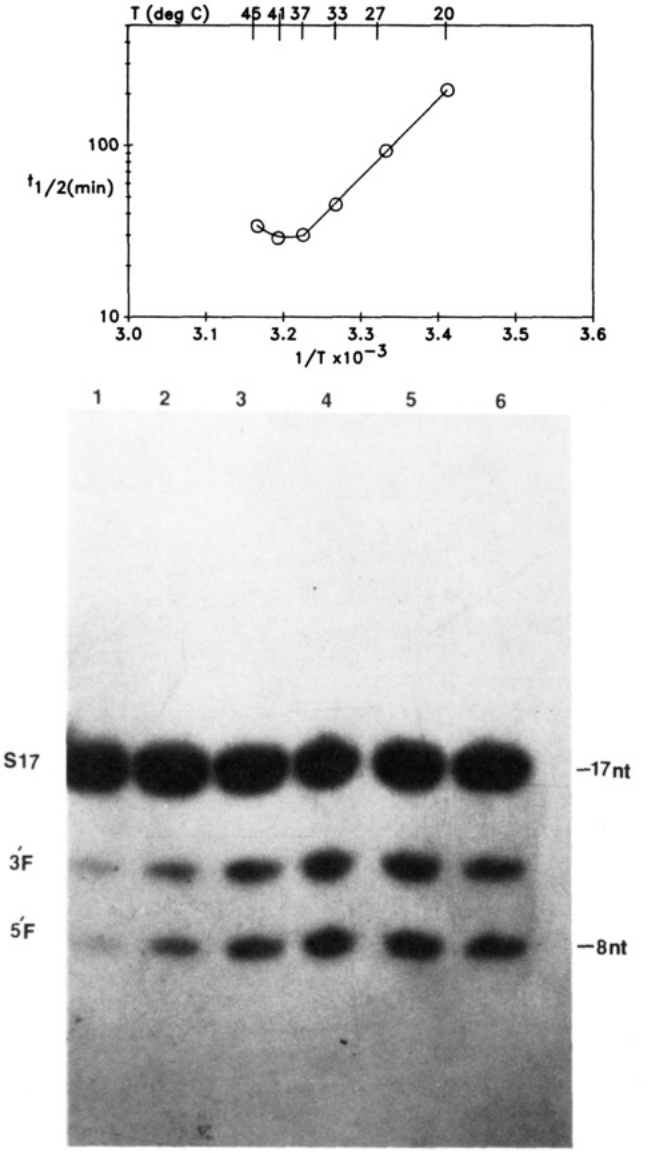

FIGURE 4: Temperature dependence of the rate of cleavage of substrate RNA S17 by catalytic RNA R51. The reaction was carried out in 12 mM $MgCl_2$, 2 mM spermidine, and 40 mM Tris, pH 7.5, at 20 (lane 1), 27 (lane 2), 33 (lane 3), 37 (lane 4), 41 (lane 5), and 45 °C (lane 6). The concentrations used were [R51] = 0.0016 μM and [S17] = 0.04 μM. R51 was unlabeled. The velocities in the graph were calculated by use of time points of 8 and 16 min. The data in the gel show the 16-min time point.

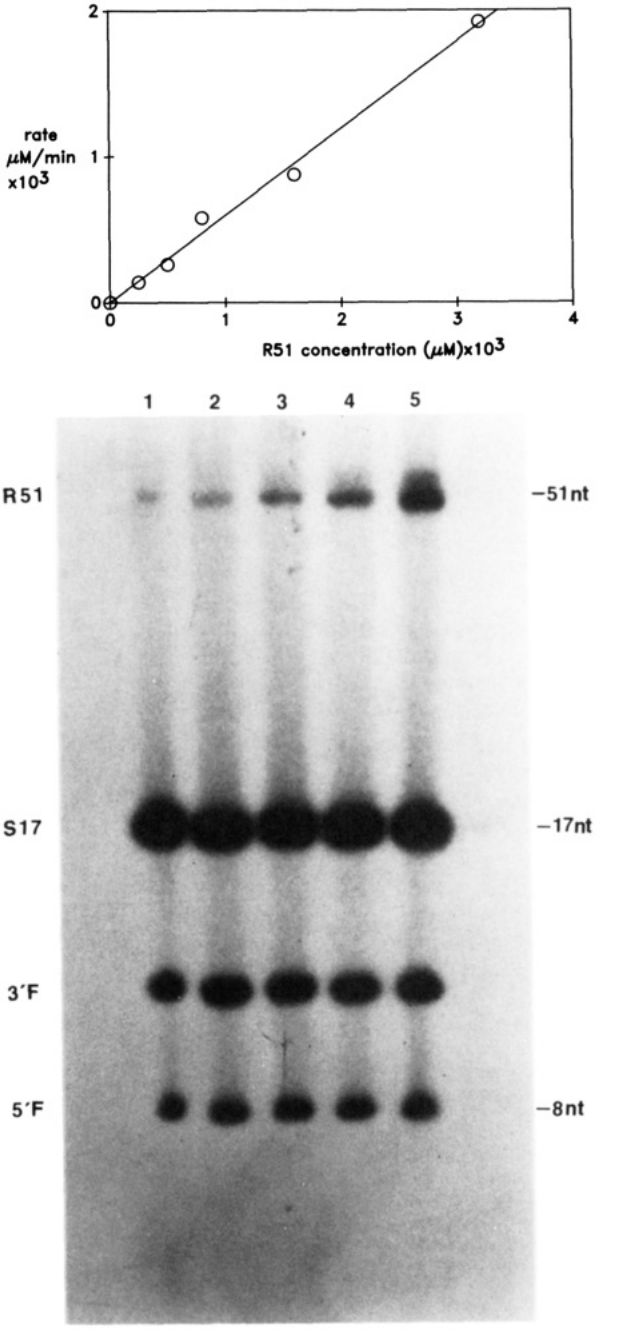

FIGURE 5: Rate of cleavage of substrate RNA S17 at varying concentrations of catalytic RNA R51. The concentration of substrate used was 0.04 μM. The reaction was carried out at 37 °C in 12 mM $MgCl_2$, 2 mM spermidine, and 40 mM Tris, pH 7.5, at [R51] = 0.25 nM for 20 and 40 min (lane 1 is the 40-min time point), at [R51] = 0.5 nM for 20 and 40 min (lane 2 is the 40-min time point), at [R51] = 0.8 nM for 10 and 20 min (lane 3 is the 20-min time point), at [51] = 1.6 nM for 5 and 10 min (lane 4 is the 10-min time point), and at [R51] = 3.2 nM for 2.5 and 5 min (lane 5 is the 5-min time point).

The reaction follows Michealis–Menten-type kinetics with initial velocity being dependent upon substrate concentration at a constant RNA catalyst concentration. The results of this type of experiment are shown in Figure 3 with the data plotted in an Eadie–Hofstee graph. The slope of this graph gives a K_m of 0.03 μM, which is a very small K_m for RNA-catalyzed reactions, and a turnover number k_{cat} = 2.1/min. This turnover number is comparable to that of other RNA-catalyzed reactions.

The reaction showed a temperature dependence similar to that which would be expected of a reaction involving base-paired RNA molecules. The slope of the Arrhenius plot shown in Figure 4 begins to fall of at 37 °C. A very rapid rate of reduction in rate of reaction was seen above 41 °C, and this is consistent with a melting out of the catalytic RNA structure. At 50 °C no reaction was detectable. The reaction rate at temperatures below 37 °C showed a linear reciprocal temperature dependence consistent with a classical lowering of the energy of activation for the reaction. The slope of the line in the Arhennius plot for temperatures of 37 °C and below gave an energy of activation of 19 kcal/mol, which is close to that found for the hammerhead cleavage mechanism of 13.1 kcal/mol (Uhlenbeck, 1987). The larger energy of activation for this cleavage may be due to alternative structures that may exist during the course of the reaction.

The reaction rate at saturating substrate concentrations is linear with increasing RNA catalyst concentration as one would expect for a true catalytic reaction. Figure 5 shows the results of this experiment. The RNA catalyst R51 is not

destroyed during the course of the reaction but instead continues to react in an unaltered state.

The above experiments were also carried out with a shorter 10-base substrate RNA sequence, 5′-GACAGUCCUG-3′. This substrate RNA, however, was less efficient than the substrate having 14 bases of satellite RNA. The 10-base substrate RNA had a K_m = 0.06 μM and k_{cat} = 0.8/min (data not shown) and was therefore not regarded as having the optimal number of satellite RNA bases.

Discussion

The short catalytic RNA sequences described in this paper have not previously been shown to be catalytic. Upon comparing them with other catalytic RNA sequences (Cech, 1987), we find no similarity between these and other catalytic RNA molecules. This is even true when we compare the (−)sTRSV catalytic/substrate sequences with the catalytic centers of viroid, virusoid, and satellite RNA molecules, which produce products containing 2′,3′-cyclic phosphates and 5′-OH termini. The common catalytic domain seen within these RNA molecules is the so-called hammerhead structure (Forster & Symons, 1987). In addition to being able to fold into the hammerhead motif, these hammerhead catalytic complexes all have 13 specific bases as part of four consensus sequences in common (Uhlenbeck, 1987). The sequences we identified as the catalytic center of (−)sTRSV contain none of these consensus sequences.

The hammerhead model for RNA cleavage has been well documented, and detailed kinetics for RNA cleavage have been determined by Uhlenbeck (1987). A comparison of the properties of RNA catalysis by the hammerhead with those of the RNA-catalyzed reaction described in this paper shows both similarities and differences. Both reactions produce products terminating in 2′,3′-cyclic phosphate and 5′-OH, and the dependences of the reaction rate on pH and Mg^{2+} concentration were virtually identical.

Temperature dependence was quite different. The hammerhead structure gave a temperature optimum of 55 °C while for the reaction described herein this temperature optimum was 37 °C. The energy of activation for this reaction is 19 kcal/mol as compared to that of the hammerhead catalytic reaction of 13 kcal/mol. Very likely, alternative structures exist for the catalysis itself. The turnover number for the hammerhead catalytic RNA was 0.5/min at 55 °C. This is compared to 2.1/min at 37 °C for the catalytic center of (−)sTRSV as described in this paper. The K_m value was 0.62 μM for the hammerhead at 55 °C as compared to 0.03 μM in our study with the (−)sTRSV catalytic center. It can be seen that the K_m for the reaction described herein is 20 times smaller. If one divides the value for k_{cat}/K_m for (−)sTRSV by that for k_{cat}/K_m for the hammerhead catalytic structure, the ratio is 87. This value represents the relative efficiency of the two catalytic centers and argues that the catalytic center of (−)sTRSV is catalytically the most efficient.

Acknowledgments

We are most grateful for information and advice provided us by Jamal Buzayan, who suggested an RNA substrate as small as 10 bases might serve as a substrate. We thank Paul Feldstein, George Bruening, Olke Uhlenbeck, Robert Symons, and Wayne Gerlach for helpful comments and advice at various stages of this work and Margaret Hicks for RNA folding.

References

Bruening, G., Buzayan, J., Gerlach, W., & Hampel, A. (1988) in *Proteins to Ribosomes*, Vol. 1, *Structure and Expression* (Sarma, R. H., & Sarma, M. H., Eds.) pp 239–248, Adenine Press, New York.

Buzayan, J. M., Gerlach, W. L., Bruening, G., Keese, P., & Gould, A. R. (1986a) *Virology 151*, 186–199.

Buzayan, J. M., Gerlach, W. L., & Bruening, G. (1986b) *Nature 323*, 349–352.

Buzayan, J. M., Hampel, A., & Bruening, G. (1986c) *Nucleic Acids Res. 14*, 9729–9743.

Cech, T. R. (1987) *Science 236*, 1532–1539.

Devereux, J., Haeberli, P., & Smithies, O. (1984) *Nucleic Acids Res. 12*, 387–395.

Donis-Keller, H., Maxam, A. M., & Gilbert, W. (1977) *Nucleic Acids Res. 4*, 2527–2538.

Epstein, L. M., & Gall, J. G. (1987) *Cell 48*, 535–543.

Forster, A., & Symons, R. (1987) *Cell 49*, 211–220.

Gerlach, W. L., Buzayan, J. M., Schneider, I. R., & Bruening, G. (1986) *Virology 151*, 172–185.

Milligan, J., Groebe, D. R., Witherell, G., & Uhlenbeck, O. (1987) *Nucleic Acids Res. 15*, 8783–8798.

Sharmeen, L., Kuo, M., Dinter-Gottlieb, G., & Taylor, J. (1988) *J. Virol. 62*, 2674–2679.

Uhlenbeck, O. (1987) *Nature 328*, 596–600.

Zucker, M., & Stiegler, P. (1981) *Nucleic Acids Res. 9*, 133.